inventions

Article

Parametric Open Source Cold-Frame Agrivoltaic Systems

Joshua M. Pearce [1,2]

[1] Department of Electrical & Computer Engineering, Western University, London, ON N6A 5B9, Canada; joshua.pearce@uwo.ca
[2] Ivey Business School, Western University, London, ON N6G 0N1, Canada

Abstract: There is an intense need to optimize agrivoltaic systems. This article describes the invention of a new testing system: the parametric open source cold-frame agrivoltaic system (POSCAS). POSCAS is an adapted gardening cold-frame used in cold climates as it acts as a small greenhouse for agricultural production. POSCAS is designed to test partially transparent solar photovoltaic (PV) modules targeting the agrivoltaic market. It can both function as a traditional cold frame, but it can also be automated to function as a full-service greenhouse. The integrated PV module roof can be used to power the controls or it can be attached to a microinverter to produce power. POSCAS can be placed in an experimental array for testing agricultural and power production. It can be easily adapted for any type of partially transparent PV module. An array of POSCAS systems allows for the testing of agrivoltaic impacts from the percent transparency of the modules by varying the thickness of a thin film PV material or the density of silicon-based cells, and various forms of optical enhancement, anti-reflection coatings and solar light spectral shifting materials in the back sheet. All agrivoltaic variables can be customized to identify ideal PV designs for a given agricultural crop.

Keywords: additive manufacturing; agriculture; agrivoltaic; distributed manufacturing; farming; gardening; open hardware; photovoltaic; recycling; solar energy

Citation: Pearce, J.M. Parametric Open Source Cold-Frame Agrivoltaic Systems. *Inventions* **2021**, *6*, 71. https://doi.org/10.3390/inventions6040071

Academic Editor: Umberto Lucia

Received: 23 September 2021
Accepted: 24 October 2021
Published: 26 October 2021

1. Introduction

Seemingly relentless cost declines [1,2], brought on by an aggressive industrial learning curve [3–5], have been the standard in the solar photovoltaic (PV) industry for the last several decades. PV costs are expected to continue to decline by another 60% in the next decade [6]. Even without these future reductions in cost, any scale of PV from residential to industrial, is currently lower than the net-metered cost of grid electricity [7–9]. PV costs have dropped so low they can even be used in conjunction with heat pumps to profitably electrify heating and replace natural gas use in the U.S. and Canada [10]. These economic realities demonstrate that fossil fuel-fired electricity is no longer competitive, and solar energy via PV electrical production is now normally the least costly electricity source [11,12]. Even ignoring the slated PV cost reductions from additional scaling and manufacturing efficiency gains, there are several PV technical improvements which are likely to become widespread in the next decade, such as black silicon, which increases silicon-based PV production by improving optical enhancement [13,14], or bifacial PV, which absorbs light from the backside of the module [15,16]. It can thus be expected that PV costs will continue to decline, and that PV will continue to be the most rapid growing source of electricity production, and gain electrical market share [17]. In 2018, PV had 505 GW, or 2% of global electricity production [18]. By 2019 it had increased to 627 GW [19] and in 2020 added more than 106 GW of additional capacity [20].

This PV growth is great news for the environment because PV are substantial net energy producers [21] and as PV efficiencies have steadily climbed [22], PV can pay their energy back in a year [23]. This large PV growth, however, comes with challenges. First, high population density cities, where the majority of humanity now live [24], lack adequate surface area for PV to meet electrical needs even when ignoring heating and transportation electrification. Thus, massive surface areas are needed for PV, which are normally found in rural areas [25] where most agricultural production occurs. This drives land use conflicts for continued PV growth. These siting conflicts were once relegated to wind farm development [26–29], but are becoming a major issue with large-scale PV projects as they can interfere with food production [30–33]. With the human population increasing 1.15% per year [34], food production will have to increase by 70% from 2005 to 2050 to feed the expected 9.1 billion people [35]. Past conversion of crop land to energy (i.e., ethanol) production increased food costs and thus global hunger [36–39]. Fortunately, agrivoltaics, which involve the strategic co-development of land for both PV electrical generation and agriculture, can meet growing energy and food demands simultaneously without conflict [40–42]. Agrivoltaics have the potential to increase global land productivity by 35–73% [40], while minimizing agricultural displacement for energy [42–44]. Agrivoltaics are under intense research investigation including: aloe vera [45], aquaponics (aquavoltaics) [46], corn/maize [47,48], lettuce [49,50], grapes [51], and wheat [52]. Many of these studies showed either marginal impacts on crop production or an increase (i.e., shade tolerant crops and leafy vegetables like lettuce prefer partial shading from PV [53]). Dual-use of land for both PV and agriculture generates a mutually beneficial partnership [54–56] and is supported both by farmers [57] and the PV industry [58].

Agrivoltaic optimization, however, has hardly begun. Studies normally focus on a single crop and test the basic geometry of the PV systems. Yet, the globe has over 20,000 species of edible plants [59] and PV systems have numerous variables that could alter agrivoltaic production including: (i) array geometry and racking, (ii) type of module, (iii) type of PV material, (iv) transparency of module, (v) spectral transmission of module including the impact of optical enhancement techniques such as anti-reflection coatings (ARCs) and (vi) the use of spectral shifting materials within the module. The number of permutations can be overwhelming. Thus, comparative studies often focus on the use of many small PV systems (e.g., a few modules in one ground mounted rack). This has the disadvantage of introducing a large number of edge effects as the crops are exposed to direct sunlight early and late in the day in the experimental systems, but not in hectare-scaled production. To overcome these challenges, a method is needed to provide low-cost agrivoltaic testing and optimization for research in this burgeoning field.

This study reports on the invention of a new testing system: the parametric open-source cold-frame agrivoltaic system (POSCAS). POSCAS is an adaptation of a standard gardening cold-frame used in cold climates as it acts as a small greenhouse for agricultural production. In a POSCAS, the glazing of the cold frame is replaced with a semi-transparent PV module in order to test it for use in the agrivoltaic market. In order to minimize costs for agrivoltaic experimentation, the POSCAS is designed for distributed recycling and additive manufacturing (DRAM). First, the parametric script-based design of the POSCAS frame will be discussed. Next, the method of manufacture will be outlined and the economic costs of production will be calculated. Sensitivity analyses will be run on all major design variables. Then, the use of the POSCAS to perform agrivoltaic experimental design will be demonstrated with a case study. Finally, future work, markets, and the automation of the invention will be outlined in order to identify ideal PV designs for a given agricultural crop.

2. Materials and Methods

In order to minimize the cost of production to make the technology as accessible as possible and thus accelerate agrivoltaic experimentation, POSCAS is designed to be an open hardware device using best practices [60–62]. It is thus compliant with the Open Source Hardware Association's definition of open hardware [63]. The documentation and the source code are licensed under GNU General Public License (GNU GPL v3) [64], the hardware is licensed under CERN Open Hardware License Version 2—Strongly Reciprocal (CERN-OHL-S) [65] and this article is Creative Commons Attribution (CC-By) [66].

2.1. Parametric Frame Design

There are hundreds of types of PV modules already, and the industry can be expected to have a much wider range, in terms of materials and sizes, in the future. In order to ensure that the POSCAS system is as widely usable as possible and future proof, it was designed to be parametric so that it can be adapted for any size of PV module and designed to take advantage of distributed manufacturing. For the frame, the thickness of the walls, type of wall insulation, possessing a floor or being directly located on the ground, the tilt angle of the module can all be controlled by a parametric OpenSCAD script housed at the Open Science Framework [67]. OpenSCAD version 2019.05 is a free and open source script based solid modeling program [68]. The script outputs a 3-D printable file (STL) so the frame body can be manufactured from waste plastic using distributed recycling and additive manufacturing (DRAM) techniques [69–71].

2.2. Using DRAM to Fabricate a POSCAS

Open source waste plastic extruders (i.e., recyclebots) upcycle post-consumer plastic waste into 3-D printing filament to be used in conventional fused filament 3-D printers [72]. Now recyclebots can be mounted on 3-D printers themselves for direct printing with fused filament fabrication [73]. The open source 3-D printing community, having democratized additive manufacturing with the Self-Replicating Rapid Prototyper (RepRap) project [74–76], has enthusiastically embraced open source methods to recycle 3-D printing waste [77]. At this point, there have been demonstrations of DRAM for the following thermopolymers:

- Polyethylene terephthalate (PET) alone [78,79] and with blends with styrene ethylene butylene styrene (SEBS) and maleic anhydride (MA) compatibilizers [80];
- High-density polyethylene (HDPE) [81–83];
- Polypropylene (PP) [73,83];
- Polystyrene (PS) [83];
- Polylactic acid (PLA) [28–31];
- Linear low density polyethylene (LLDPE) / low density polyethylene (LDPE) [84];
- Acrylonitrile butadiene styrene (ABS) [69,85–88];
- Polycarbonate (PC) [89];
- Thermoplastic polyurethane (TPU) [90];
- Polylactic acid (PLA) [91–94]; and
- Polymer composites using carbon-reinforced plastic [95], fiber-filled composites [96,97], various types of waste wood [98,99] and acrylonitrile styrene acrylate (ASA) composites [100].

This provides considerable material flexibility for producing the components of the POSCAS as well as their accessibility, as most labs would have ready access to many of these types of thermoplastics.

DRAM can be used to radically reduce the cost of products as the material costs a fraction of conventional costs of equivalent products [101–103]. To calculate the material cost of the base model of the POSCAS (C_{POSCAS}) Equation (1) is used:

$$C_{POSCAS} = m \times c_{wp} + f \tag{1}$$

where m is the mass of the frame (kg), c_{wp} is the cost of processing the waste plastic ($/kg) and f is the cost of the fasteners. In this study, the mass of the plastic frame is determined with CURA v 4.11.0 [104], an open source slicing program for a range of infill parameters. A sensitivity was run on this cost of ASA from (1) commercial filament costs from Amazon $30/kg [105]; (2) commercial pellets $8/kg [106]; (3) recycled commercial pellets $2.50/kg [107]; and (4) DRAM $0.025/kg [72]. ASA was selected as an example polymer here because of its UV stability and weather resistance [108,109]. For the lowest cost and simplest system, heavy duty marine grade nylon cable zip ties were selected as fasteners. Cable zip ties are used on the top side of the module frame, connecting it to the structural frame of the POSCAS. The UV resistant black zip ties are 8.5 mm wide (about half of the average mounting hole in standard PV aluminum frames, 355 mm long, have a tensile strength rating of 54 kg, and cost $0.09 a piece [110]. The zip ties are fabricated with industrial strength UV resistant nylon 6/6 that is Type 21 UL listed to withstand temperatures from −40 to 85 °C. The number of fasteners needed depends on the module manufacturer. For example, Longi, the highest volume PV manufacturer in 2020, has six mounting holes per side of a module for their Hi-MO 5 bifacial modules [111] while Heliene's 144 M10 bifacial module has 4 mounting holes per side [112]. Each of the M10 modules is made up of 6 rows of 24 or 144 half wafer cells.

2.3. Agrivoltaic Module Experimental Design with a POSCAS

Although conventional PV modules have been used in agrivoltaics, the POSCAS is designed to test the performance of semi-transparent agrivoltaic specific PV modules. There are two primary types of semi-transparent PV that have mostly been used for building integrated PV(BIPV): (i) thin-film based semi-transparent PV, where in general the thickness of the active layer is adjusted to impact the transparency of the module and (ii) modules using crystal silicon technology where the spacing between cells is adjusted to adjust transparency [113–117]. This latter method also includes crystalline-silicon spherical solar microcells [118]. The experimental matrices are shown in Figure 1. For thin films, as shown in Figure 1a, the matrix can be generated by incrementing the RGB color and, as as shown in Figure 2, a white-black OpenSCAD script also housed in the Open Science Framework [67] was written to arrange cells following the input parameters summarized in Table 1.

There are other variations of the patterns shown in Figure 1b. For example, reversing the numbers of parameters a and b in the script result in the variations shown in Figure 2 for a 33% covered (67% transparent) agrivoltaic PV module.

Figures 1b and 2 were made with the spacing between cell locations in the module being fixed, but this variable can also be changed resulting in larger spaces between the cells and higher percent transmission of light for the plants. Changing this variable enables any transmission value and a vast array of different aesthetics (e.g., lines or blocks or PV). This represents yet another sensitivity, which underscores the importance of low-cost POSCAS manufacturing (e.g., just to fully investigate a single plant species for the arrays in Figure 1, 18 systems would be needed and more than that if arrangement of cells would be further explored). This level of optimization has not been reported in the literature.

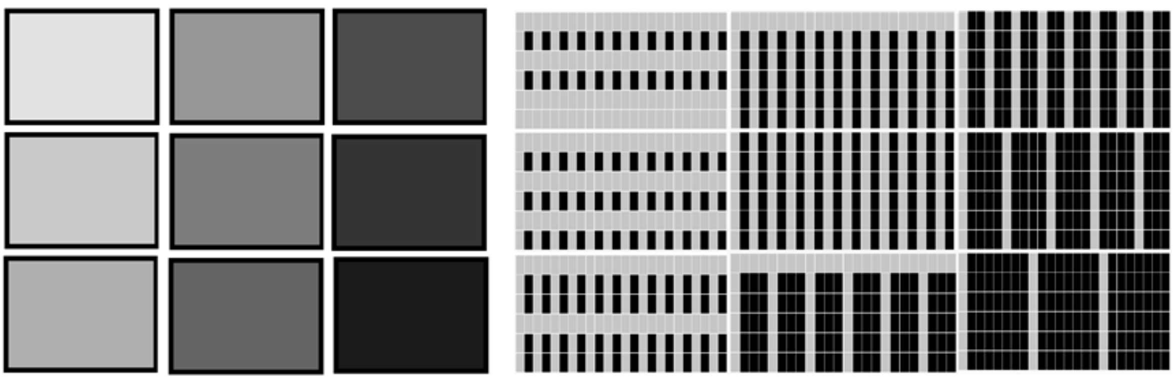

(a) (b)

Figure 1. Semitransparent PV experimental matrices from 10% to 90% transparency in 10% increments for: (**a**) thin film PV; (**b**) crystalline silicon-based PV cell separation.

Table 1. Approximate percent of PV coverage per module with factor a and b in darkwhite.scad script [67].

Approximate Percent PV	a	b
10 *	2	2 *
20	2	2
30	2/3	3/2
40	2	6
50	2	0
60	4	6
70	6	6
80	5	0
90	8	0

*—row.

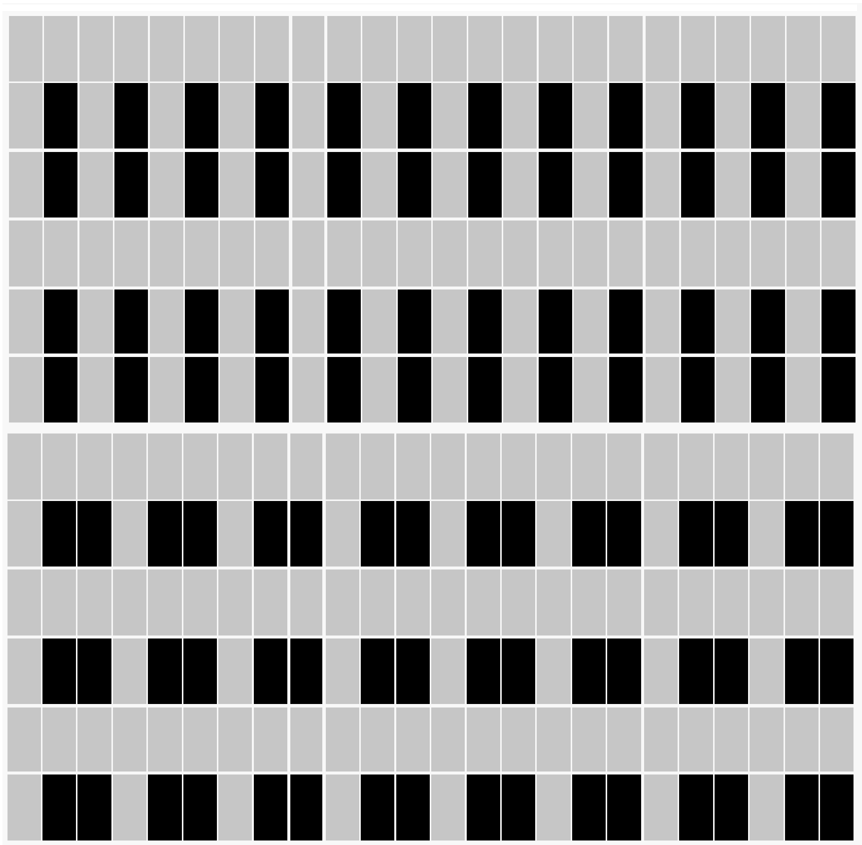

Figure 2. Semitransparent PV with 33% covered agrivoltaic panel using parameters 2/3 (**top**) and 3/2 (**bottom**) for a/b.

3. Results

3.1. Parametric Frame Design

A parametric script was successfully developed in OpenSCAD with several features for optimization of the POSCAS design shown in Figure 3 with the automatic customizer enabled. First, although the examples shown here are based around a specific module [112], the dimensions of the module are controlled by three variables (lpv, wpv, tpv) that can be easily adjusted. The depth of the box can also be controlled by a single variable so that the POSCAS can be heightened for taller crops or act as a raised bed. The variables are shown and defined in Table 2 that determine the POSCAS geometry. Note that the sp and tc variables are not shown, as they would be determined by the module manufacturer and are only included in the script for visualization purposes.

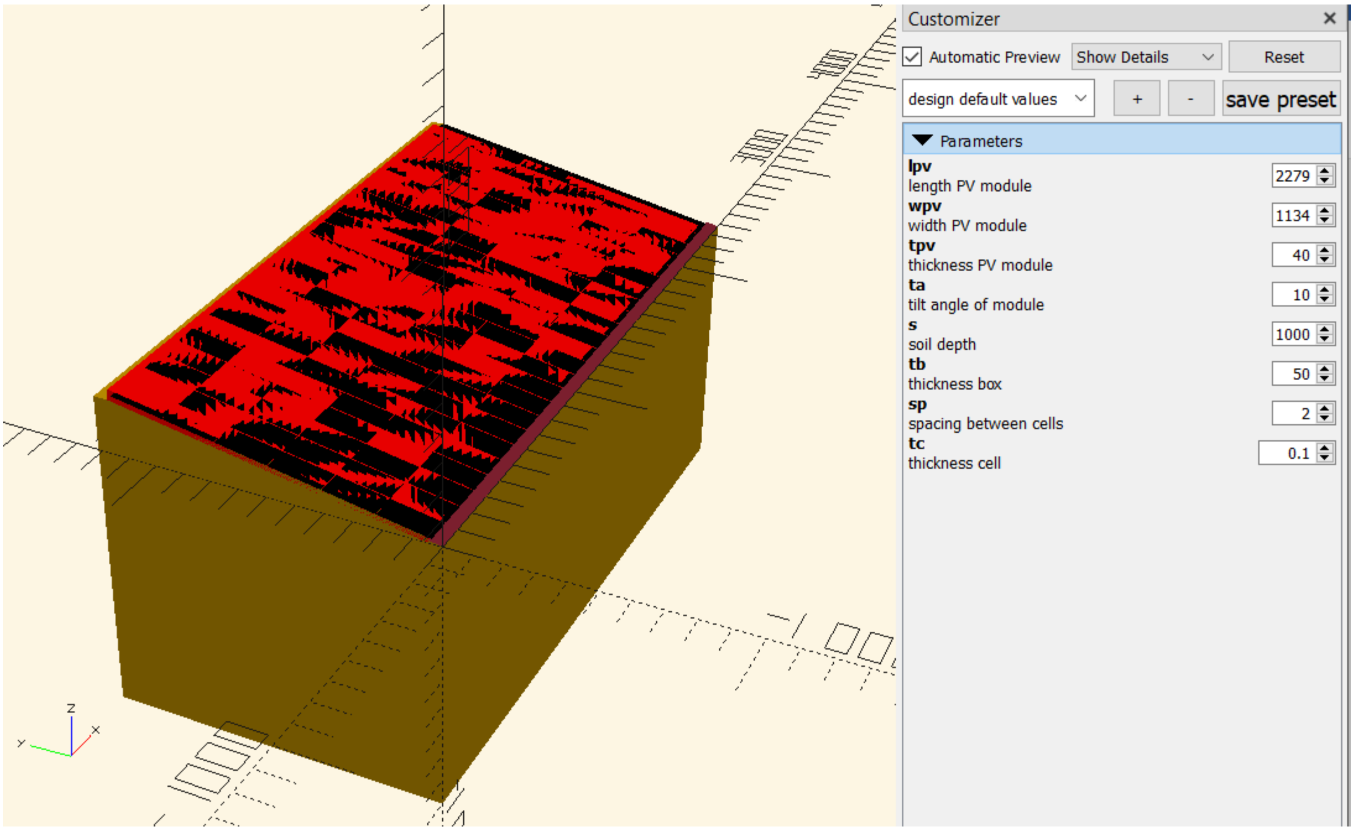

Figure 3. Basic POSCAS design with semitransparent PV, a 10-degree tilt angle, and a box depth of 1m shown with the automatic customizer in OpenSCAD.

Table 2. Primary POSCAS variables in OpenSCAD that determine 3-D printable box geometry.

Variable	Unit	Explanation
lpv	mm	Length of the PV module to be adjusted for PV based on specification sheet from PV manufacturer.
wpv	mm	Width of the PV module to be adjusted for PV based on specification sheet from PV manufacturer.
tpv	mm	Thickness of the PV to be adjusted for PV based on specification sheet from PV manufacturer.
ta	$\circ$	Tilt angle of the modules measured from the ground surface. This can be optimized for solar electric yield based on latitude.
s	mm	This determines the height of the walls of the POSCAS, which provides the maximum soil depth for a raised bed growing system.
tb	mm	Box wall thickness will depend on the loads expected and the materials used to fabricate the POSCAS.

Next, the tilt angle (ta) can be adjusted to optimize the PV electricity production based on the latitude of the installation. Adjusting the tilt angle automatically resizes the box to ensure the module still fits, as shown in Figure 4.

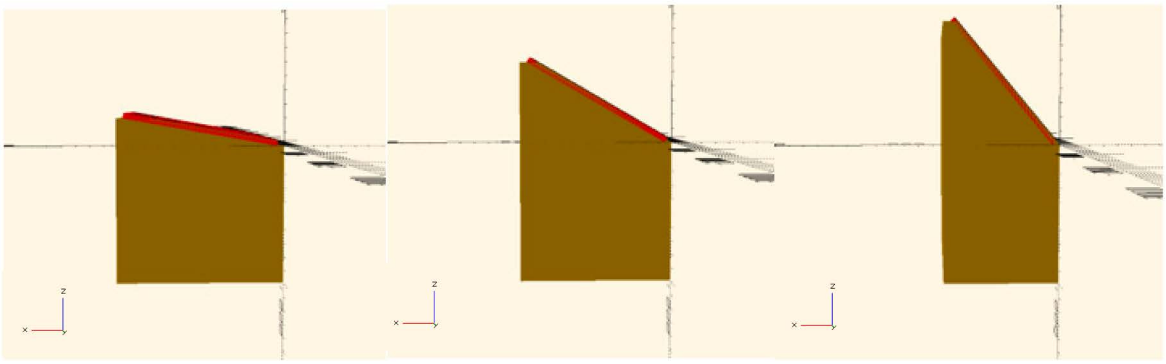

(**a**) (**b**) (**c**)

Figure 4. The impact of varying the tilt angle on POSCAS geometry: (**a**) 10, (**b**) 30 and (**c**) 50 degrees.

The POSCAS default design does not have a bottom, and can be placed directly on the soil for plant growth (Figure 5a). This minimizes plastic use for fabrication. In the case where the POSCAS array may be set up in areas with no or poor soil (e.g., a parking lot) the POSCAS design can also be adjusted to have a bottom, and thus be used more like a planter (Figure 5b).

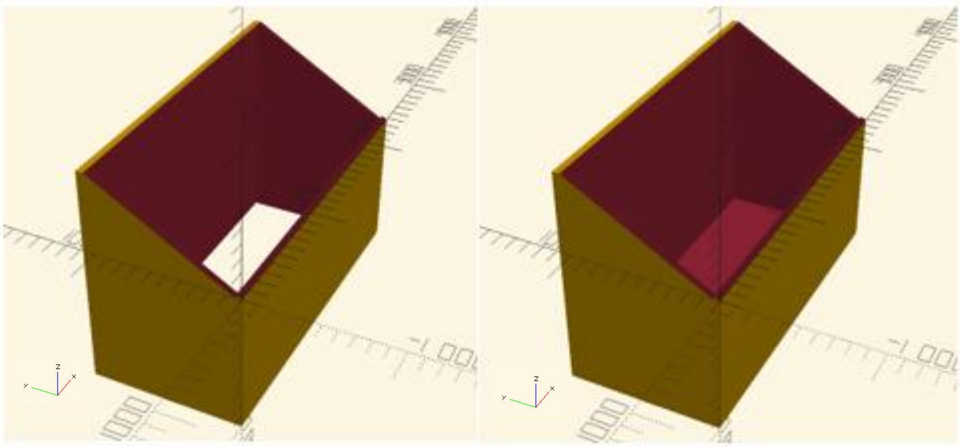

(**a**) (**b**)

Figure 5. Interior of the POSCAS (**a**) with no bottom and (**b**) with a bottom.

After the fabrication of the POSCAS base, depending on the method of manufacture, holes are located on the back (high end) of the base to attach the PV module to it through its mounting holes, with the cable zip ties. If using AM, these holes can be added to the OpenSCAD. If using any other method or if the same base is being used for different PV module manufacturers, the necessary mounting holes can be drilled out.

3.2. DRAM-Based POSCAS Economics

Several DRAM-manufactured economic sensitivities were performed on the POSCAS design: (1) polymer cost, (2) bottom/bottomless, (3) tilt angle, (4) soil depth, (5) wall thickness and (6) module hole type. The base economic case used DRAM for production, a tilt angle of 30 degrees, soil depth of 500 mm, box wall thickness of 50 mm, and 4 zip ties with the slicing parameters 20% infill and 2.4 mm out shell walls. All economic values are given in 2021 U.S. dollars. It should also be noted that all of these costs are material costs alone, and do not include labor costs for fabrication. The invention also does not include the cost of the PV module as the POSCAS is meant to test different types of PV modules. The total cost including potential module costs will be discussed for other applications.

The results of these sensitivities are shown in Table 3. First, it is clear from Table 3 that the most important parameter is the source of raw materials. The material costs of the base POSCAS model range from almost $1000 for commercial 3-D printing filament to $8.19 for the use of distributed recycling and additive manufacturing. These lower costs for DRAM are consistent with other studies in the literature [101–103]. Changing the tilt angle has a much smaller effect on the costs (e.g., less than 10% difference going from a tilt angle of 30 to 50 degrees). More shallow tilt angles have lower costs because less plastic is used in the wedge. This effect is minimized with a deep POSCAS as a greater fraction of the POSCAS's mass comes from the vertical walls. Wall thickness also has a substantial impact on the material costs of the POSCAS. The economic impacts of needing additional cable zip ties are minimal as, even with 6 mounting holes per module side, they still represent less than 10% of the cost of the lowest cost DRAM manufacturing base case, as can be seen in Table 3. Adding a bottom to the base case of the POSCAS increases its costs by 36% as the mass increases from 30.5 kg to 44.9 kg. Even in this case, the entire material cost for the POSCAS is under US$12.

Table 3. Economic sensitivities of POSCAS production; all values in US$. Bold values are the base POSCAS case.

Polymer Type	Feedstock Cost ($/kg)	Frame Mass Bottomless (kg)	Frame Cost Bottomless POSCAS ($)	Total Cost Bottomless POSCAS ($)	Percentage Difference Base POSCAS
Commercial Filament	30	30.5	915.00	915.56	196%
Commercial Pellets	8	30.5	244.00	244.56	187%
Recycled Pellets	2.5	30.5	76.25	76.81	161%
DRAM	**0.25**	**30.5**	**7.63**	**8.19**	0%
Tilt Angle (degrees)					
10	0.25	24.2	6.05	6.61	21%
30	0.25	30.5	7.63	8.19	0%
50	0.25	33.5	8.38	8.94	9%
Soil Depth (mm)					
1000	0.25	49.7	12.43	12.99	45%
500	0.25	30.5	7.63	8.19	0%
250	0.25	20.8	5.20	5.76	35%
Infill (%)					
0	0.25	9.5	2.38	2.94	94%
10	0.25	20.0	5.00	5.56	38%
20	0.25	30.5	7.63	8.19	0%
50	0.25	62.0	15.50	16.06	65%
100	0.25	114.3	28.58	29.14	112%
Wall thickness (mm)					
10	0.25	18.8	4.70	5.26	44%
20	0.25	30.5	7.63	8.19	0%
50	0.25	66.5	16.63	17.19	71%
Box Type					
Bottomless	0.25	30.5	7.63	8.19	0%
Bottom	0.25	44.9	11.23	11.79	36%
Module hole type	**Cost of zip ties**	**Percent Cost**			
4	0.36	4.4%			
6	0.54	6.6%			

Lastly, one of the main advantages of the DRAM method is the ability to control the interior design of a product. This is done by controlling the infill percent in the slicing of the STL. Table 3 shows the impact of both increasing and decreasing the percentage infill from the base case of 20% for the POSCAS. This has a radical impact on the economics. If manufactured solid (i.e., 100% infill) the costs increase to over US$29 but drop to $5.56 for 10% fill. To visualize the impact of the infill on the structure of the POSCAS the solid and partial infill cases are shown in Figure 6 using Cura slicing screenshots of the lower left-hand corner of the POSCAS in mid 3-D print. In Figure 6 the red layers represent the external shell, green is the inner wall, orange is the infill, which is yellow in the 100% case as every layer is treated as a top/bottom layer.

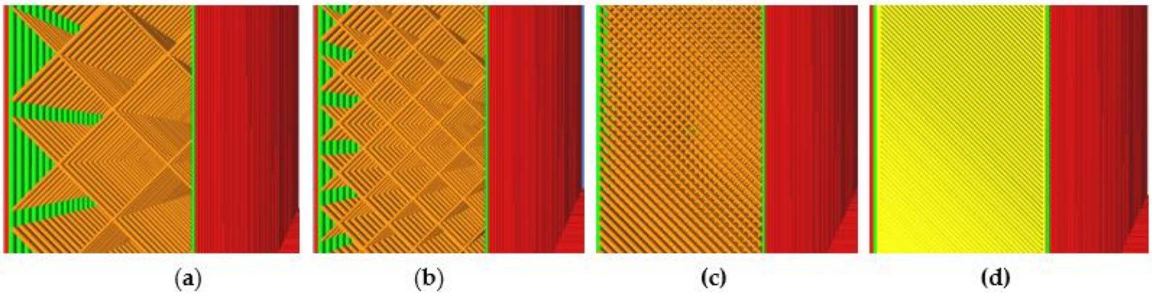

Figure 6. Cura slicing screenshots of the lower left-hand corner of the POSCAS varying the infill density (**a**) 10%, (**b**) 20%, (c) 50% and (**d**) 100%. The red layers are external shell, green is the inner wall, and orange is the infill, which is yellow in the 100% case as every layer is treated as a top/bottom layer.

3.3. Case Study of Red Agrivoltaic Module Experimental Design with a POSCAS

In addition to simple, partially transparent PV, researchers have begun to experiment on partially transparent PV with colored designs for aesthetic reasons [119]. This approach may also be of use in agrivoltaic applications. Already Li et al., have been integrating semi-transparent PV into greenhouses [120–122]. It is well established that tinted semi-transparent PV can actually increase yields for some plants [123]. There is research that has shown spectral shifting materials could also be of use in greenhouses [124–126].

The use of the POSCAS to perform agrivoltaic experimental design is demonstrated with a case study of such spectral shifting. POSCAS can be used to optimize Heliene greenhouse solar panels [127] for specific crops. Such Heliene red modules can have different transparencies by adjusting the density of the crystalline-silicon based cells (i.e., in Figure 1b). They are bifacial PV modules which generate electricity both from the top where sunlight strikes it directly on the exterior of the greenhouse and from any reflection coming from the albedo inside the greenhouse on a red-colored back-sheet. The back sheet spectrally shifts the green region of the light spectrum, which is normally reflected from plants, into red light that can be absorbed by plants. Such spectral shifting can increase greenhouse production [128]. This makes the modules appear red wherever there is not a cell. At the same time, some of this light is reflected back to the PV cell, which can be used to reduce the electrical use of the greenhouse. Large trials are underway on this technology where a large single greenhouse has been outfitted with enhanced red BIPV modules where one type of plant (basil) is studied (i.e., collecting basil plant height, chlorophyll content, fresh and dry weight at harvest, as well as climate and light quality data in the greenhouse during the growing cycle) [129,130]. This setup has 66 kW of identical enhanced bifacial red PV modules. In addition to the transmission percentage (Figure 1) for these crystalline silicon-based PV, the enhancements of red greenhouse modules have many other variables to optimize for, including testing the density, size and chemical makeup of nanoparticles responsible for the spectral shifting via fluorescence [131–133]. The interplay between the PV and these nanoparticles need to be investigated for each new crop. POSCAS can be deployed in arrays where a single module can be used for each variable, so the 66 kW used experimentally for basil to test one type of PV could instead be used to perform at least 100 of these permutations, as shown in Figure 7. This would use the same number of PV modules and allow for testing 10 different plant species and 10 different spectral shifting materials simultaneously in a version of large-scale combinatorial experimentation. Similarly, it could be used for testing 10 variables against a control (e.g., glass) and nine of the transparencies outlined in Figure 1 for the PV modules can be used in the array (Figure 7).

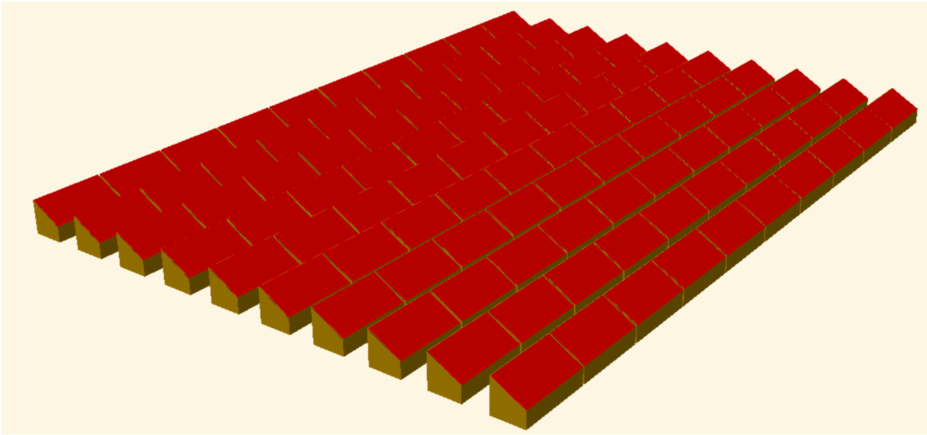

Figure 7. A 10 by 10 array of POSCAS to be used for combinatorial experimentation on agrivoltaic systems.

Finally, costs can be further reduced by sharing the backside of a POSCAS in a double system as shown in Figure 8.

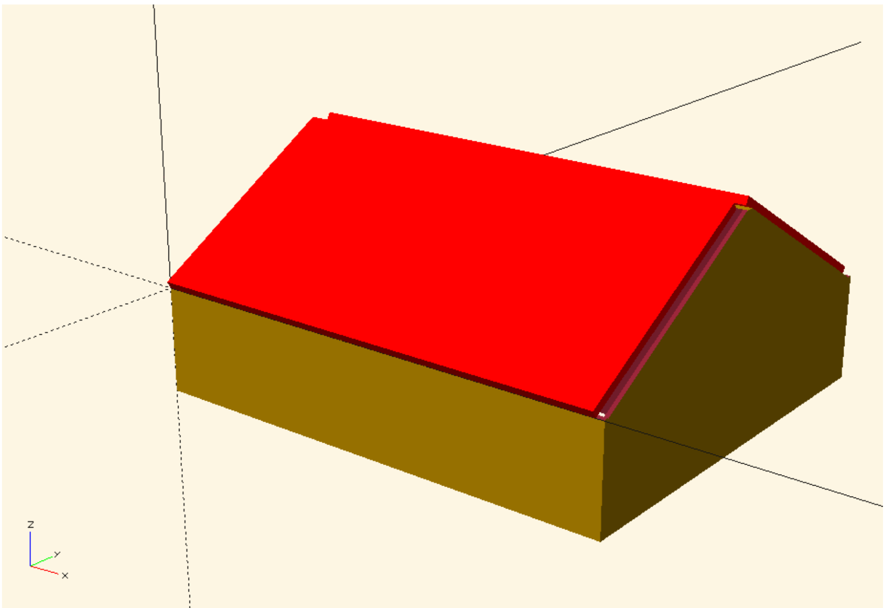

Figure 8. A Double POSCAS design.

The double POSCAS design is made with the following OpenSCAD module:

```
module doubleposcas(){
    poscas();
    translate([0,2*wb,0])mirror([0,1,0])poscas();
}
```

This effectively makes the back side of each of the halves of the double POSCAS use the same wall. As shown in Figure 9.

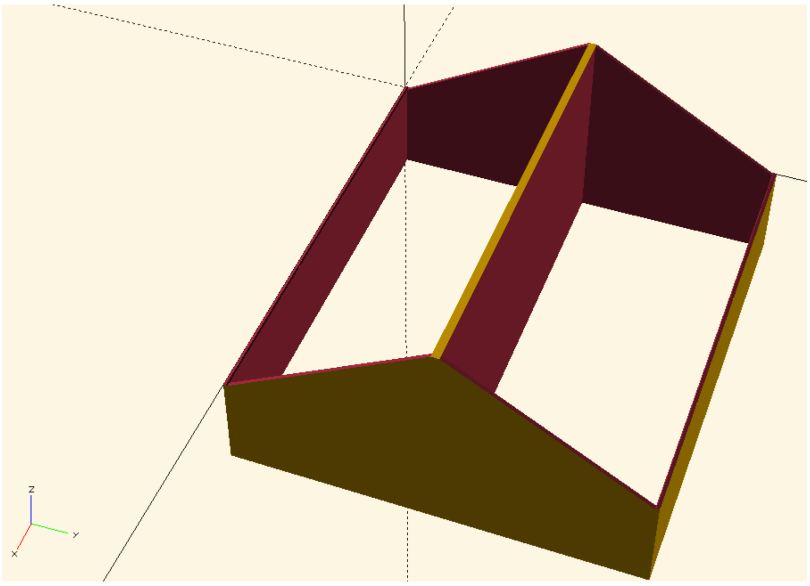

Figure 9. Internal view double bottomless double POSCAS.

Thus, the mass per PV module can be reduced. The Cura-estimated mass of the bottomless POSCAS is 9.5kg, equivalent to 9.5kg/PV module. The Cura-estimated mass of the double-bottomless POSCAS design is 14.6kg, which is 7.3kg/ PV module because back wall can be shared. These double POSCAS devices can be used in an E-W facing arrays as shown in Figure 10.

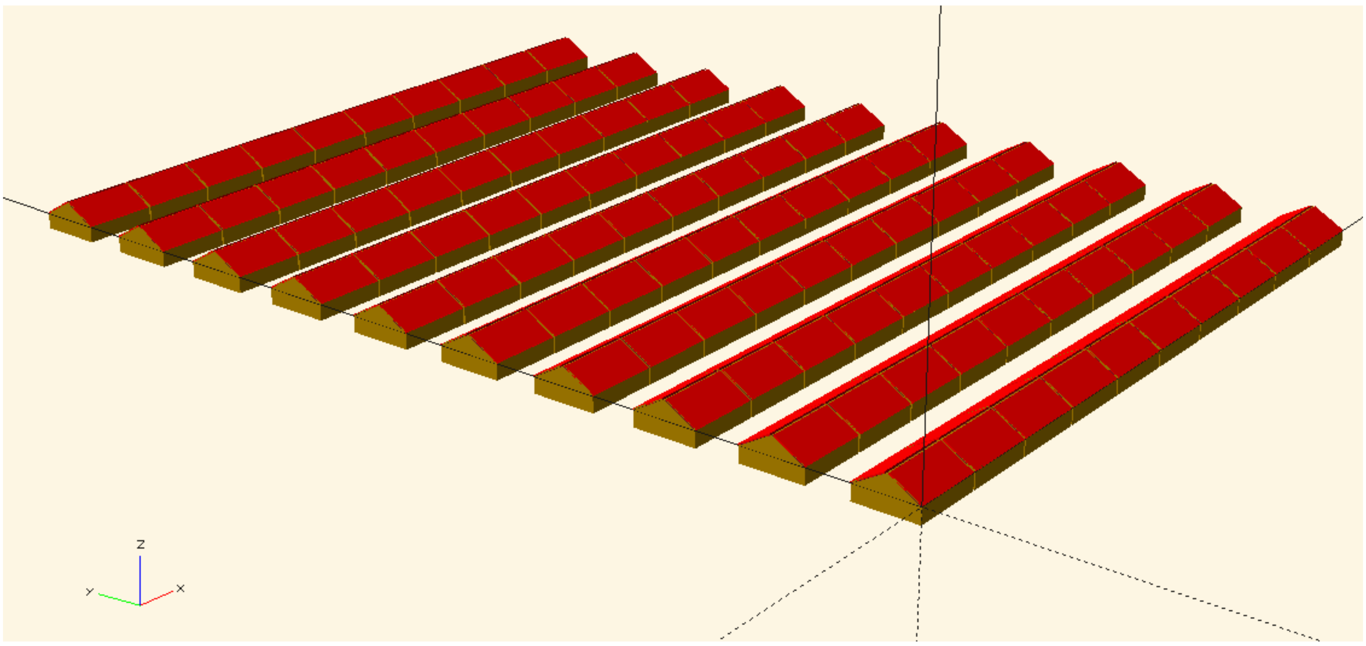

Figure 10. Array of double POSCAS facing E-W with tilt angle of 30 degrees.

4. Discussion

4.1. Comparison to Cold Frames

Typical commercial cold frames constructed from glass or plastic window layers and wood or metal structural components range in cost from \$100 to \$250. PV modules range in cost from about \$0.20–\$0.60/W and have powers per module between 250 W to 550 W. This results in PV module costs between \$50 and \$330. With the POSCAS costing from about $9 to $1000 depending on material choice, a cold-frame equivalent could cost less than 60% of a commercial cold frame or up to 5 times the most expensive cold frame. These costs are dominated by the PV module costs. At the same level of production, it is expected that partially transparent PV should be less costly per module than conventional PV because thin films are generally less costly and an agrivoltaic module based on crystalline silicon technology would use fewer solar cells. This indicates that, even on direct comparison to cold frames alone using only cold frame functionality, POSCAS may be economically competitive.

It should be pointed out that some commercial cold frames have a means to keep the roof up while working on the crops. This can be done with any short pole or an open source adjustable window support adapted from an open source greenhouse design [134] shown in Figure 11. This design is also conducive to DRAM and needs the addition of some basic fasteners. The STL files that make up the mount that is normally screwed into a wood cold frame can be directly integrated into the POSCAS frame. This addition will make the POSCAS functionally equivalent to the highest cost commercial cold frames and yet has material costs that can be substantially lower using lower-cost partially transparent PV modules.

Figure 11. Open source adjustable window support [134].

4.2. Comparison to Ground-Mounted PV Racks

Comparing the POSCAS to cold frames is not straightforward, as the POSCAS has the potential to generate renewable electricity, whereas commercial cold frames offer no other value creation opportunities. In addition, if the PV have been enhanced, as in the example case study of Heliene red PV modules, the agricultural yield also has the potential to increase, creating additional value over the clear windows used in commercial cold frames. The POSCAS-generated solar electricity can be directly grid connected with a microinverter or, if in an array as in Figure 7, can use microinverters or string inverters like a conventional PV system using a conventional rack.

For this functionality, it is more instructive to compare the POSCAS to conventional PV racking. Conventional proprietary ground-mounted PV racks range in cost from $0.19–0.44/W [135], so if the same range of PV module power is used as discussed above, this cost is $47.50 to $242.00 per module. These values can be directly compared to the material costs of the POSCAS. To be completely equivalent it should be compared to the POSCAS with a base so that the soil that the plants are growing in can be used as ballast. A DRAM base with a bottom costs less than $12 (Table 3), indicating that the POSCAS is an extremely inexpensive method of DIY PV racking. For a company to mass manufacture POSCAS the material costs would be closer to the costs of recycled pellets ($76.81 by Table 3), indicating there is the potential for profit while still falling within the current price range of conventional racks. Again, however, the POSCAS provides added value as conventional PV racks do not operate as cold frames (e.g., extend the growing season of crops in cold climates). In addition, the POSCAS would be expected to enjoy the synergistic benefits of conventional agrivoltaics and the ability to easily customize them for a specific application provides the opportunity to optimize for solar electric generation value. So, for example, an E-W facing array made possible by the double POSCAS would be appropriate for electric grids that are being challenged to meet demand in the late afternoon [136].

4.3. POSCAS for Agrivoltaic Research

The POSCAS provides more value than a cold frame or a PV rack alone. The open source parametric script provided here allows for making modifications in the framework of the POSCAS to do many experiments. For example, they can be used to test the impact of insulation in cold frames on growth of a range of crops using identical covers/modules. Fabricating the POSCAS with zero percent infill allows for adding insulation using, for example, spray in foam insulation. The POSCAS designs allow for varying the gap available for insulation by changing the width of the walls of the frame. In addition, it is possible to leverage past work on 3-D printed truss-like lattice non-stochastic structures for sandwich panels [137] for the walls of the POSCAS. This architecture could be integrated into the POSCAS design to have an optimal strength/mass ratio making up the walls.

The value of the ability of many POSCAS to be used in an experimental array should be stressed. The parametric design allows researchers to rapidly customize the POSCAS or array of POSCASs for a given experiment follow the examples above. By using many individual POSCAS, tests can be performed by varying the thickness of a thin film PV material or the density of silicon-based cells, and various forms of optical enhancement, anti-reflection coatings and solar light spectral shifting materials in the back sheet. For experiments monitoring the performance of the PV module in a POSCAS, either commercial microconverters or a wide range of open source power monitoring systems can be used [138–141]. In this way, a POSCAS using an open source microcontroller for standard off-the-shelf sensors can replace much more costly approaches [142,143]. For researchers considering studies on agrivoltaic modules, the DRAM POSCAS is clearly the most economical option.

4.4. Future Work

This article analyzed the design, manufacturing, and economics of the POSCAS invention. The results were both technically and economically promising, indicating rich areas of future work. First, the original intended purpose of the POSCAS is to test PV modules for agrivoltaic applications. There is considerable future work to be done in manufacturing large numbers of POSCAS in order to identify ideal PV designs for as many agricultural crops as are of interest to agrivoltaic markets. Second, the POSCAS is well positioned technically to be automated (i.e., become a smart cold frame). Using the same open source hardware design process as was used for the mechanical members here, future work could integrate a temperature sensor, fan and/or a motor to control air inflow into the greenhouse box to regulate its temperature using an Arduino microcontroller based on previous open source designs [144–147]. It can also be coupled to any number of other sensors to automate the care of the plants by controlling, for example, irrigation and fertilization.

Agricultural sensors that could be integrated into the POSCAS in the future are numerous. First, low-cost digital cameras can be used for a number of applications and can be mounted on the POSCAS frame and powered with the PV. These cameras can either be used to replace other optical sensors or work in conjunction with them. These cameras can be used to detect weeds, and for disease detection and diagnosis to either be analyzed by experts or machine vision/AI. These same cameras can be used to monitor leaf color and can be coupled to soil sensors to determine optimal fertilization and water. The cameras can monitor soil images and be coupled with pH and electrochemical sensors to maintain optimum soil conditions. These same cameras can again be used for determining the leaf areas and brightness to help optimize watering and/or control irrigation. Lastly, the camera images can be used to determine crop harvest readiness, for example by either size or color for the ripeness of fruits or vegetables. This, again, could be automated with machine vision and AI to be used for automated yield monitoring. Other sensors include those like airflow sensors to measure soil air permeability and other types of soil properties, including compaction, soil structure, and moisture levels. These data can also be used to create mathematical models for soil porous soil structures for controlled experiments [148]. Another method to get soil moisture is to measure the dielectric constant in the soil. Similarly, tensiometers and other mechanical sensors could be integrated to detect the force used by the roots in water absorption to guide/control irrigation.

These many sensors could be integrated into an agricultural open source Internet of things (IoT) [149,150] where many POSCAS could provide for data aggregation across a wide geographic area to bring timely, actionable information to small farmers and gardeners regarding seeding, weeding, fertilizing, watering, and harvesting. The POSCAS data could also be coupled to remote satellite sensing and open source weather station data and processed with AI and machine learning to optimize both crop and PV production.

Finally, this invention provides a research opportunity to experimentally verify the albedo from the crops and their impacts on the different types of partially-transparent bifacial PV modules. This may also be important for optimizing the agricultural component of agrivoltaic arrays.

5. Conclusions

This article has reported on the design of a parametric open source cold-frame agrivoltaic system. The parametric nature of the design enables the POSCAS geometry to be customized for any form of agricultural crop and agrivoltaic system. It can operate directly on the soil, or as a grow box placed on a sterile surface. The tilt angle can be adjusted for any latitude. The POSCAS enables research for agrivoltaic optimization by altering (i) array geometry and racking, (ii) type of module, (iii) type of PV material, (iv) transparency of module, (v) spectral transmission of module including the impact of optical enhancement techniques such as ARCs, and (vi) the use of spectral shifting materials within the module. The POSCAS is designed for distributed recycling and additive manufacturing, which was found here to be the least expensive material cost based on the method of manufacturing. It can be manufactured in this way from any waste thermoplastic. The POSCAS design can also be lower in cost of both commercial cold frames and small-scale ground mounted PV racking. Finally, the POSCAS is an open source device and other researchers are encouraged to build, test and modify it for the benefit of humanity.

6. Open Source Hardware Certification

This invention will be submitted for OSHWA certification.

Funding: This research was supported by the Thompson Endowment.

Data Availability Statement: All data and designs are available in Parametric Open-Source Smart Cold-Frame Agrivoltaic System. 2021. Available online: https://osf.io/k6xwv/ accessed on (25 October 2021); The registration is available at: https://osf.io/acf7h accessed on (25 October 2021).

Conflicts of Interest: The author declares no conflict of interest.

References

1. Feldman, D.; Barbose, G.; Margolis, R.; Wiser, R.; Darghouth, N.; Goodrich, A. *Photovoltaic (PV) Pricing Trends: Historical, Recent, and Near-Term Projections*; National Renewable Energy Laboratory: Golden, CO, USA, 2012.
2. Barbose, G.L.; Darghouth, N.R.; Millstein, D.; LaCommare, K.H.; DiSanti, N.; Widiss, R. *Tracking the Sun X: The Installed Price of Residential and Non-Residential Photovoltaic Systems in the United States*; Lawrence Berkley National Laboratory: Berkeley, CA, USA, 2017.
3. Yu, C.F.; van Sark, W.G.J.H.M.; Alsema, E.A. Unraveling the photovoltaic technology learning curve by incorporation of input price changes and scale effects. *Renew. Sustain. Energy Rev.* **2011**, *15*, 324–337. [CrossRef]
4. Hong, S.; Chung, Y.; Woo, C. Scenario analysis for estimating the learning rate of photovoltaic power generation based on learning curve theory in South Korea. *Energy* **2015**, *79*, 80–89. [CrossRef]
5. Mauleón, I. Photovoltaic learning rate estimation: Issues and implications. *Renew. Sustain. Energy Rev.* **2016**, *65*, 507–524. [CrossRef]

6. Reuters. Solar Costs to Fall Further, Powering Global Demand—Irena. Reuters. 2017. Available online: https://www.reuters.com/article/singapore-energy-solar-idUSL4N1MY2F8 (accessed on 7 April 2020).
7. Lai, C.S.; McCulloch, M.D. Levelized cost of electricity for solar photovoltaic and electrical energy storage. *Appl. Energy* **2017**, *190*, 191–203. [CrossRef]
8. Kang, M.H.; Rohatgi, A. Quantitative analysis of the levelized cost of electricity of commercial scale photovoltaics systems in the US. *Sol. Energy Mater. Sol. Cells* **2016**, *154*, 71–77. [CrossRef]
9. Richard, C. New Wind and Solar Cheaper Than Existing Coal and Gas. 2018. Available online: http://www.windpowermonthly.com/article/1491146 (accessed on 7 April 2020).
10. Pearce, J.M.; Sommerfeldt, N. Economics of Grid-Tied Solar Photovoltaic Systems Coupled to Heat Pumps: The Case of Northern Climates of the U.S. and Canada. *Energies* **2021**, *14*, 834. [CrossRef]
11. IRENA. *Renewable Power Generation Costs in 2017*; IRENA: Abu Dhabi, United Arab Emirates, 2018.
12. Dudley, D. Renewable Energy Will Be Consistently Cheaper than Fossil Fuels By 2020, Report Claims. Forbes 2018. Available online: https://www.forbes.com/sites/dominicdudley/2018/01/13/renewable-energy-cost-effective-fossil-fuels-2020/ (accessed on 7 April 2020).
13. Kroll, M.; Otto, M.; Käsebier, T.; Füchsel, K.; Wehrspohn, R.; Kley, E.B.; Tünnermann, A.; Pertsch, T. Black silicon for solar cell applications. In *Photonics for Solar Energy Systems IV*; International Society for Optics and Photonics: Brussels, Belgium, 2012; Volume 8438. [CrossRef]
14. Modanese, C.; Laine, H.; Pasanen, T.; Savin, H.; Pearce, J. Economic Advantages of Dry-Etched Black Silicon in Passivated Emitter Rear Cell (PERC) Photovoltaic Manufacturing. *Energies* **2018**, *11*, 2337. [CrossRef]
15. Liang, T.S.; Pravettoni, M.; Deline, C.; Stein, J.S.; Kopecek, R.; Singh, J.P.; Luo, W.; Wang, Y.; Aberle, A.G.; Khoo, Y.S. A review of crystalline silicon bifacial photovoltaic performance characterisation and simulation. *Energy Environ. Sci.* **2019**, *12*, 116–148. [CrossRef]
16. Burnham, L.; Riley, D.; Walker, B.; Pearce, J.M. Performance of bifacial photovoltaic modules on a dual-axis tracker in a high-latitude, high-albedo environment. In Proceedings of the 2019 IEEE 46th Photovoltaic Specialists Conference (PVSC), Chicago, IL, USA, 16 June 2019; pp. 1320–1327.
17. Barron, A. Cost reduction in the solar industry. *Mater. Today* **2015**, *18*, 2–3. [CrossRef]
18. Center for Climate and Energy Solutions (CECS). Renewable Energy. 2019. Available online: https://www.c2es.org/content/renewable-energy/ (accessed on 11 November 2020).
19. IEA. Snapshot of Global PV Markets 2020 Report IEA-PVPS T1-37. 2020. Available online: https://iea-pvps.org/wp-content/uploads/2020/04/IEA_PVPS_Snapshot_2020.pdf (accessed on 11 November 2020).
20. IEA. Solar PV—Renewables 2020—Analysis. Available online: https://www.iea.org/reports/renewables-2020/solar-pv (accessed on 20 September 2021).
21. Pearce, J.; Lau, A. Net Energy Analysis For Sustainable Energy Production From Silicon Based Solar Cells. In Proceedings of the American Society of Mechanical Engineers Solar 2002: Sunrise on the Reliable Energy Economy, Reno, NV, USA, 15–20 June 2002.
22. NREL. Best Research-Cell Efficiency Chart. Available online: https://www.nrel.gov/pv/cell-efficiency.html (accessed on 12 January 2021).
23. Bhandari, K.P.; Collier, J.M.; Ellingson, R.J.; Apul, D.S. Energy payback time (EPBT) and energy return on energy invested (EROI) of solar photovoltaic systems: A systematic review and meta-analysis. *Renew. Sustain. Energy Rev.* **2015**, *47*, 133–141. [CrossRef]
24. Engelke, P. *Foreign Policy for an Urban World: Global Governance and the Rise of Cities*; Atlantic Council: Washington DC, USA, 2013.
25. Denholm, P.; Margolis, R.M. Land-use requirements and the per-capita solar footprint for photovoltaic generation in the United States. *Energy Policy* **2008**, *36*, 3531–3543. [CrossRef]
26. Wüstenhagen, R.; Wolsink, M.; Bürer, M.J. Social acceptance of renewable energy innovation: An introduction to the concept. *Energy Policy* **2007**, *35*, 2683–2691. [CrossRef]
27. Sovacool, B. Exploring and Contextualizing Public Opposition to Renewable Electricity in the United States. *Sustainability* **2009**, *1*, 702–721. [CrossRef]
28. Sovacool, B.K.; Ratan, P.L. Conceptualizing the acceptance of wind and solar electricity. *Renew. Sustain. Energy Rev.* **2012**, *16*, 5268–5279. [CrossRef]
29. Batel, S.; Devine-Wright, P.; Tangeland, T. Social acceptance of low carbon energy and associated infrastructures: A critical discussion. *Energy Policy* **2013**, *58*, 1–5. [CrossRef]
30. Calvert, K.; Mabee, W. More solar farms or more bioenergy crops? Mapping and assessing potential land-use conflicts among renewable energy technologies in eastern Ontario, Canada. *Appl. Geogr.* **2015**, *56*, 209–221. [CrossRef]
31. Calvert, K.; Pearce, J.M.; Mabee, W.E. Toward renewable energy geo-information infrastructures: Applications of GIScience and remote sensing that build institutional capacity. *Renew. Sustain. Energy Rev.* **2013**, *18*, 416–429. [CrossRef]
32. Nonhebel, S. Renewable energy and food supply: Will there be enough land? *Renew. Sustain. Energy Rev.* **2005**, *9*, 191–201. [CrossRef]
33. Dias, L.; Gouveia, J.P.; Lourenço, P.; Seixas, J. Interplay between the Potential of Photovoltaic Systems and Agricultural Land Use. *Land Use Policy* **2019**, *81*, 725–735. [CrossRef]
34. UN Department of Economic and Social Affairs. *Concise Report on the World Population Situation in 2014*; UN: New York, NY, USA, 2014.

35. FAO. How to Feed the World 2050. 2009; Retrieved 3 December 2020. Available online: http://www.fao.org/fileadmin/templates/wsfs/docs/Issues_papers/HLEF2050_Global_Agriculture.pdf (accessed on 25 October 2021).
36. Runge, C.F.; Senauer, B. How Biofuels Could Starve the Poor. *Foreign Aff.* **2007**, *86*, 41.
37. Tomei, J.; Helliwell, R. Food versus Fuel? Going beyond Biofuels. *Land Use Policy* **2016**, *56*, 320–326. [CrossRef]
38. Thompson, P.B. The Agricultural Ethics of Biofuels: The Food vs. Fuel Debate. *Agriculture* **2012**, *2*, 339–358. [CrossRef]
39. Tenenbaum, D.J. Food vs. Fuel: Diversion of Crops Could Cause More Hunger. *Environ. Health Perspect.* **2008**, *116*, A254–A257. [CrossRef] [PubMed]
40. Dupraz, C.; Marrou, H.; Talbot, G.; Dufour, L.; Nogier, A.; Ferard, Y. Combining solar photovoltaic panels and food crops for optimising land use: Towards new agrivoltaic schemes. *Renew. Energy* **2011**, *36*, 2725–2732. [CrossRef]
41. Dinesh, H.; Pearce, J.M. The potential of agrivoltaic systems. *Renew. Sustain. Energy Rev.* **2016**, *54*, 299–308. [CrossRef]
42. Mavani, D.D.; Chauhan, P.M.; Joshi, V. Beauty of Agrivoltaic System regarding double utilization of same piece of land for Generation of Electricity & Food Production. *Int. J. Sci. Eng. Res.* **2019**, *10*, 118–148.
43. Mow, B. Solar Sheep and Voltaic Veggies: Uniting Solar Power and Agriculture. 2018. Available online: https://www.nrel.gov/state-local-tribal/blog/posts/solar-sheep-and-voltaic-veggies-uniting-solar-power-and-agriculture.html (accessed on 2 July 2020).
44. Adeh, E.H.; Good, S.P.; Calaf, M. Solar PV Power Potential is Greatest Over Croplands. *Sci. Rep.* **2019**, *9*, 11442. [CrossRef]
45. Ravi, S.; Macknick, J.; Lobell, D.; Field, C.; Ganesan, K.; Jain, R.; Elchinger, M.; Stoltenberg, B. Colocation opportunities for large solar infrastructures and agriculture in drylands. *Appl. Energy* **2016**, *165*, 383–392. [CrossRef]
46. Pringle, A.M.; Handler, R.M.; Pearce, J.M. Aquavoltaics: Synergies for dual use of water area for solar photovoltaic electricity generation and aquaculture. *Renew. Sustain. Energy Rev.* **2017**, *80*, 572–584. [CrossRef]
47. Amaducci, S.; Yin, X.; Colauzzi, M. Agrivoltaic systems to optimize land use for electric energy production. *Appl. Energy* **2018**, *220*, 545–561. [CrossRef]
48. Sekiyama, T.; Nagashima, A. Solar Sharing for Both Food and Clean Energy Production: Performance of Agrivoltaic Systems for Corn, A Typical Shade-Intolerant Crop. *Environments* **2019**, *6*, 65. [CrossRef]
49. Marrou, H.; Wery, J.; Dufour, L.; Dupraz, C. Productivity and radiation use efficiency of lettuces grown in the partial shade of photovoltaic panels. *Eur. J. Agron.* **2013**, *44*, 54–66. [CrossRef]
50. Elamri, Y.; Cheviron, B.; Lopez, J.M.; Dejean, C.; Belaud, G. Water budget and crop modelling for agrivoltaic systems: Application to irrigated lettuces. *Agric. Water Manag.* **2018**, *208*, 440–453. [CrossRef]
51. Malu, P.R.; Sharma, U.S.; Pearce, J.M. Agrivoltaic potential on grape farms in India. *Sustain. Energy Technol. Assess.* **2017**, *23*, 104–110. [CrossRef]
52. Marrou, H.; Guilioni, L.; Dufour, L.; Dupraz, C.; Wéry, J. Microclimate under agrivoltaic systems: Is crop growth rate affected in the partial shade of solar panels? *Agric. For. Meteorol.* **2013**, *177*, 117–132. [CrossRef]
53. Riaz, M.H.; Imran, H.; Alam, H.; Alam, M.A.; Butt, N.Z. Crop-Specific Optimization of Bifacial PV Arrays for Agrivoltaic Food-Energy Production: The Light-Productivity-Factor Approach. *arXiv* **2021**, arXiv:2104.00560.
54. Santra, P.; Pande, P.C.; Kumar, S.; Mishra, D.; Singh, R.K. Agri-voltaics or Solar farming- the Concept of Integrating Solar PV Based Electricity Generation and Crop Production in a Single Land use System. *Int. J. Renew. Energy Res.* **2017**, *7*, 694–699.
55. Guerin, T.F. Impacts and opportunities from large-scale solar photovoltaic (PV) electricity generation on agricultural production. *Environ. Qual. Manag.* **2019**, *28*, 7–14. [CrossRef]
56. Barron-Gafford, G.A.; Pavao-Zuckerman, M.A.; Minor, R.L.; Sutter, L.F.; Barnett-Moreno, I.; Blackett, D.T.; Thompson, M.; Dimond, K.; Gerlak, A.K.; Nabhan, G.P.; et al. Agrivoltaics provide mutual benefits across the food–energy–water nexus in drylands. *Nat. Sustain.* **2019**, *2*, 848–855. [CrossRef]
57. Pascaris, A.S.; Schelly, C.; Pearce, J.M. A First Investigation of Agriculture Sector Perspectives on the Opportunities and Barriers for Agrivoltaics. *Agronomy* **2020**, *10*, 1885. [CrossRef]
58. Pascaris, A.S.; Schelly, C.; Burnham, L.; Pearce, J.M. Integrating Solar Energy with Agriculture: Industry Perspectives on the Market, Community, and Socio-Political Dimensions of Agrivoltaics. *Energy Res. Soc. Sci.* **2021**, *75*, 102023. [CrossRef]
59. PFAF. Edible Uses. Available online: https://pfaf.org/user/edibleuses.aspx (accessed on 20 September 2021).
60. Gibb, A. *Building Open Source Hardware: DIY Manufacturing for Hackers and Makers*; Pearson Education: London, UK, 2014.
61. Pearce, J.M. *Open-Source Lab: How to Build Your Own Hardware and Reduce Research Costs*; Elsevier: Amsterdam, The Netherlands, 2014.
62. Oberloier, S.; Pearce, J.M. General Design Procedure for Free and Open-Source Hardware for Scientific Equipment. *Designs* **2018**, *2*, 2. [CrossRef]
63. Open Source Hardware Association. Definition (English). Available online: https://www.oshwa.org/definition/ (accessed on 20 September 2021).
64. The GNU General Public License v3.0—GNU Project—Free Software Foundation. Available online: https://www.gnu.org/licenses/gpl-3.0.en.html (accessed on 20 September 2021).
65. Cern OHL Version 2 Wiki·Projects/CERN Open Hardware Licence. Available online: https://ohwr.org/project/cernohl/wikis/Documents/CERN-OHL-version-2 (accessed on 20 September 2021).
66. Creative Commons—Attribution 2.0 Generic—CC BY 2.0. Available online: https://creativecommons.org/licenses/by/2.0/ (accessed on 20 September 2021).
67. Parametric Open-Source Cold-Frame Agrivoltaic System. 2021. Available online: https://osf.io/k6xwv/ (accessed on 20 September 2021).

68. OpenSCAD. Available online: http://openscad.org (accessed on 20 September 2021).
69. Zhong, S.; Pearce, J.M. Tightening the loop on the circular economy: Coupled distributed recycling and manufacturing with recyclebot and RepRap 3-D printing. *Resour. Conserv. Recycl.* **2018**, *128*, 48–58. [CrossRef]
70. Pavlo, S.; Fabio, C.; Hakim, B.; Mauricio, C. 3D-Printing Based Distributed Plastic Recycling: A Conceptual Model for Closed-Loop Supply Chain Design. In Proceedings of the 2018 IEEE International Conference on Engineering, Technology and Innovation (ICE/ITMC), Stuttgart, Germany, 17–20 June 2018; pp. 1–8.
71. Cruz Sanchez, F.A.; Boudaoud, H.; Camargo, M.; Pearce, J.M. Plastic recycling in additive manufacturing: A systematic literature review and opportunities for the circular economy. *J. Clean. Prod.* **2020**, *264*, 121602. [CrossRef]
72. Woern, A.L.; McCaslin, J.R.; Pringle, A.M.; Pearce, J.M. RepRapable Recyclebot: Open source 3-D prinfigure extruder for converting plastic to 3-D printing filament. *HardwareX* **2018**, *4*, e00026. [CrossRef]
73. Woern, A.L.; Byard, D.J.; Oakley, R.B.; Fiedler, M.J.; Snabes, S.L.; Pearce, J.M. Fused Particle Fabrication 3-D Printing: Recycled Materials' Optimization and Mechanical Properties. *Materials* **2018**, *11*, 1413. [CrossRef] [PubMed]
74. Sells, E.; Bailard, S.; Smith, Z.; Bowyer, A.; Olliver, V. RepRap: The Replicating Rapid Prototyper: Maximizing Customizability by Breeding the Means of Production. In *Handbook of Research in Mass Customization and Personalization*; World Scientific Publishing Company: Singapore, 2009; pp. 568–580. ISBN 978-981-4280-25-9.
75. Jones, R.; Haufe, P.; Sells, E.; Iravani, P.; Olliver, V.; Palmer, C.; Bowyer, A. RepRap—The replicating rapid prototyper. *Robotica* **2011**, *29*, 177–191. [CrossRef]
76. Bowyer, A. 3D Printing and Humanity's First Imperfect Replicator. *3D Print. Addit. Manuf.* **2014**, *1*, 4–5. [CrossRef]
77. Hunt, E.J.; Zhang, C.; Anzalone, N.; Pearce, J.M. Polymer recycling codes for distributed manufacturing with 3-D printers. *Resour. Conserv. Recycl.* **2015**, *97*, 24–30. [CrossRef]
78. Lee, J.H.; Lim, K.S.; Hahm, W.G.; Kim, S.H. Properties of recycled and virgin poly(ethylene terephthalate) blend fibers. *J. Appl. Polym. Sci.* **2013**, *128*, 1250–1256. [CrossRef]
79. Little, H.A.; Tanikella, N.G.; Reich, M.J.; Fiedler, M.J.; Snabes, S.L.; Pearce, J.M. Towards Distributed Recycling with Additive Manufacturing of PET Flake Feedstocks. *Materials* **2020**, *13*, 4273. [CrossRef] [PubMed]
80. Zander, N.E.; Gillan, M.; Burckhard, Z.; Gardea, F. Recycled polypropylene blends as novel 3D printing materials. *Addit. Manuf.* **2019**, *25*, 122–130. [CrossRef]
81. Baechler, C.; DeVuono, M.; Pearce, J.M. Distributed recycling of waste polymer into RepRap feedstock. *Rapid Prototyp. J.* **2013**, *19*, 118–125. [CrossRef]
82. Chong, S.; Pan, G.-T.; Khalid, M.; Yang, T.C.-K.; Hung, S.-T.; Huang, C.-M. Physical Characterization and Pre-assessment of Recycled High-Density Polyethylene as 3D Printing Material. *J. Polym. Environ.* **2017**, *25*, 136–145. [CrossRef]
83. Pepi, M.; Zander, N.; Gillan, M. Towards Expeditionary Battlefield Manufacturing Using Recycled, Reclaimed, and Scrap Materials. *JOM* **2018**, *70*, 2359–2364. [CrossRef]
84. Hart, K.R.; Frketic, J.B.; Brown, J.R. Recycling meal-ready-to-eat (MRE) pouches into polymer filament for material extrusion additive manufacturing. *Addit. Manuf.* **2018**, *21*, 536–543. [CrossRef]
85. Mohammed, M.I.; Wilson, D.; Gomez-Kervin, E.; Tang, B.; Wang, J. Investigation of Closed-Loop Manufacturing with Acrylonitrile Butadiene Styrene over Multiple Generations Using Additive Manufacturing. *ACS Sustain. Chem. Eng.* **2019**, *7*, 13955–13969. [CrossRef]
86. Mohammed, M.I.; Wilson, D.; Gomez-Kervin, E.; Vidler, C.; Rosson, L.; Long, J. The Recycling of E-Waste ABS Plastics by Melt Extrusion and 3D Printing Using Solar Powered Devices as a Transformative Tool for Humanitarian Aid. In Proceedings of the 29th Annual International Solid Freeform Fabrication Symposium, Austin, TX, USA, 13–15 August 2018.
87. Mohammed, M.I.; Wilson, D.; Gomez-Kervin, E.; Rosson, L.; Long, J. EcoPrinting: Investigation of Solar Powered Plastic Recycling and Additive Manufacturing for Enhanced Waste Management and Sustainable Manufacturing. In Proceedings of the 2018 IEEE Conference on Technologies for Sustainability (SusTech), Long Beach, CA, USA, 11–13 November 2018; pp. 1–6.
88. Boldizar, A.; Möller, K. Degradation of ABS during repeated processing and accelerated ageing. *Polym. Degrad. Stab.* **2003**, *81*, 359–366. [CrossRef]
89. Reich, M.J.; Woern, A.L.; Tanikella, N.G.; Pearce, J.M. Mechanical Properties and Applications of Recycled Polycarbonate Particle Material Extrusion-Based Additive Manufacturing. *Materials* **2019**, *12*, 1642. [CrossRef] [PubMed]
90. Woern, A.L.; Pearce, J.M. Distributed Manufacturing of Flexible Products: Technical Feasibility and Economic Viability. *Technologies* **2017**, *5*, 71. [CrossRef]
91. Sanchez, F.A.C.; Lanza, S.; Boudaoud, H.; Hoppe, S.; Camargo, M. Polymer Recycling and Additive Manufacturing in an Open Source context: Optimization of processes and methods. In *Annual International Solid Freeform Ffabrication Symposium, ISSF 2015*; University of Texas: Austin, TX, USA, 2015; p. 1591.
92. Cruz Sanchez, F.A.; Boudaoud, H.; Hoppe, S.; Camargo, M. Polymer recycling in an open-source additive manufacturing context: Mechanical issues. *Addit. Manuf.* **2017**, *17*, 87–105. [CrossRef]
93. Anderson, I. Mechanical Properties of Specimens 3D Printed with Virgin and Recycled Polylactic Acid. *3D Print. Addit. Manuf.* **2017**, *4*, 110–115. [CrossRef]
94. Pakkanen, J.; Manfredi, D.; Minetola, P.; Iuliano, L. About the Use of Recycled or Biodegradable Filaments for Sustainability of 3D Printing. In *Sustainable Design and Manufacturing 2017*; Campana, G., Howlett, R.J., Setchi, R., Cimatti, B., Eds.; Springer International Publishing: Cham, Switzerland, 2017; pp. 776–785.

95. Tian, X.; Liu, T.; Wang, Q.; Dilmurat, A.; Li, D.; Ziegmann, G. Recycling and remanufacturing of 3D printed continuous carbon fiber reinforced PLA composites. *J. Clean. Prod.* **2017**, *142*, 1609–1618. [CrossRef]
96. Parandoush, P.; Lin, D. A review on additive manufacturing of polymer-fiber composites. *Compos. Struct.* **2017**, *182*, 36–53. [CrossRef]
97. Heller, B.P.; Smith, D.E.; Jack, D.A. Planar deposition flow modeling of fiber filled composites in large area additive manufacturing. *Addit. Manuf.* **2019**, *25*, 227–238. [CrossRef]
98. Pringle, A.M.; Rudnicki, M.; Pearce, J.M. Wood Furniture Waste–Based Recycled 3-D Printing Filament. *For. Prod. J.* **2017**, *68*, 86–95. [CrossRef]
99. Zander, N.E. Recycled Polymer Feedstocks for Material Extrusion Additive Manufacturing. In *Polymer-Based Additive Manufacturing: Recent Developments*; ACS Symposium Series; American Chemical Society: Washington DC, USA, 2019; Volume 1315, pp. 37–51. ISBN 978-0-8412-3426-0.
100. Meyer, T.K.; Tanikella, N.G.; Reich, M.J.; Pearce, J.M. Potential of distributed recycling from hybrid manufacturing of 3-D printing and injection molding of stamp sand and acrylonitrile styrene acrylate waste composite. *Sustain. Mater. Technol.* **2020**, *25*, e00169. [CrossRef]
101. Gwamuri, J.; Wittbrodt, B.T.; Anzalone, N.C.; Pearce, J.M. *Reversing the Trend of Large Scale and Centralization in Manufacturing: The Case of Distributed Manufacturing of Customizable 3-D-Printable Self-Adjustable Glasses*; Social Science Research Network: Rochester, NY, USA, 2014.
102. Wittbrodt, B.T.; Glover, A.G.; Laureto, J.; Anzalone, G.C.; Oppliger, D.; Irwin, J.L.; Pearce, J.M. Life-cycle economic analysis of distributed manufacturing with open-source 3-D printers. *Mechatronics* **2013**, *23*, 713–726. [CrossRef]
103. Petersen, E.E.; Pearce, J. Emergence of Home Manufacturing in the Developed World: Return on Investment for Open-Source 3-D Printers. *Technologies* **2017**, *5*, 7. [CrossRef]
104. Ultimaker Cura: Powerful, Easy-to-Use 3D Printing Software. Available online: https://ultimaker.com/software/ultimaker-cura (accessed on 20 September 2021).
105. Amazon.Com: Polymaker ASA Filament 1.75mm Black ASA 1kg Spool UV Resistant ASA Filament 1.75—PolyLite ASA 3D Printer Filament: Everything Else. Available online: https://www.amazon.com/Polymaker-Printer-Filament-PolyLite-Printing/dp/B07QN4BKMJ/ (accessed on 20 September 2021).
106. ASA Pellets for Extruding Your Own Professional 3D Filament. Available online: https://www.3dxtech.com/product/asa-pellets/ (accessed on 20 September 2021).
107. Factory Sale High Temperature Resistance And High Impact Asa Plastic Granules Pellets For Lampshade And Radiator Grille—Buy Factory Sale High Temperature Resistance And High Impact Asa Granules Pellets For Lampshade And Radiator Grille, High Temperature Resistant Modified Engineering Plastic, Whether Resistance And Aging Resistance Product on Alibaba.Com. Available online: https://www.alibaba.com/product-detail/Factory-sale-high-temperature-resistance-and_1600179625457.html?spm=a2700.7724857.normal_offer.d_image.5d23e430Y78ODT (accessed on 20 September 2021).
108. McKee, G.E.; Kistenmacher, A.; Goerrissen, H.; Breulmann, M. Synthesis, Properties and Applications of Acrylonitrile–Styrene–Acrylate Polymers. In *Modern Styrenic Polymers: Polystyrenes and Styrenic Copolymers*; John Wiley & Sons, Ltd.: New York, NY, USA, 2003; pp. 341–362. ISBN 978-0-470-86721-1.
109. Massey, L.K. *The Effect of UV Light and Weather: On Plastics and Elastomers*; William Andrew: Norwhich, UK, 2006.
110. Ziptie.com 14-Inch UV Resistant Black Multi-Purpose Cable Ties, 120-Lb Tensile Strength, UL 21S Listed, 100-Pack. Available online: https://ziptie.com/14-in-120-lb-black-heavy-duty-nylon-tie-100-pack.html (accessed on 20 October 2021).
111. Hi-MO5. Available online: https://en.longi-solar.com/home/products/Hi_MO5.html (accessed on 20 September 2021).
112. Heliene 144 M10. Available online: https://heliene.com/wp-content/uploads/HELIENE_144_M10_BIFACIAL_SPEC_SSM_REV.00.pdf (accessed on 20 September 2021).
113. Leite Didoné, E.; Wagner, A. Semi-transparent PV windows: A study for office buildings in Brazil. *Energy Build.* **2013**, *67*, 136–142. [CrossRef]
114. Olivieri, L.; Caamaño-Martín, E.; Moralejo-Vázquez, F.J.; Martín-Chivelet, N.; Olivieri, F.; Neila-Gonzalez, F.J. Energy saving potential of semi-transparent photovoltaic elements for building integration. *Energy* **2014**, *76*, 572–583. [CrossRef]
115. Chae, Y.T.; Kim, J.; Park, H.; Shin, B. Building energy performance evaluation of building integrated photovoltaic (BIPV) window with semi-transparent solar cells. *Appl. Energy* **2014**, *129*, 217–227. [CrossRef]
116. Moralejo-Vázquez, F.J.; Martín-Chivelet, N.; Olivieri, L.; Caamaño-Martín, E. Luminous and solar characterization of PV modules for building integration. *Energy Build.* **2015**, *103*, 326–337. [CrossRef]
117. Martín-Chivelet, N.; Guillén, C.; Trigo, J.F.; Herrero, J.; Pérez, J.J.; Chenlo, F. Comparative Performance of Semi-Transparent PV Modules and Electrochromic Windows for Improving Energy Efficiency in Buildings. *Energies* **2018**, *11*, 1526. [CrossRef]
118. Yano, A.; Onoe, M.; Nakata, J. Prototype Semi-Transparent Photovoltaic Modules for Greenhouse Roof Applications. *Biosyst. Eng.* **2014**, *122*, 62–73. [CrossRef]
119. Yeop Myong, S.; Won Jeon, S. Design of Esthetic Color for Thin-Film Silicon Semi-Transparent Photovoltaic Modules. *Solar Energy Mater. Sol. Cells* **2015**, *143*, 442–449. [CrossRef]
120. Li, Z.; Yano, A.; Cossu, M.; Yoshioka, H.; Kita, I.; Ibaraki, Y. Electrical Energy Producing Greenhouse Shading System with a Semi-Transparent Photovoltaic Blind Based on Micro-Spherical Solar Cells. *Energies* **2018**, *11*, 1681. [CrossRef]

121. Li, Z.; Yano, A.; Cossu, M.; Yoshioka, H.; Kita, I.; Ibaraki, Y. Shading and Electric Performance of a Prototype Greenhouse Blind System Based on Semi-Transparent Photovoltaic Technology. *J. Agric. Meteorol.* **2018**, *74*, 114–122.
122. Li, Z.; Yano, A.; Yoshioka, H. Feasibility Study of a Blind-Type Photovoltaic Roof-Shade System Designed for Simultaneous Production of Crops and Electricity in a Greenhouse. *Appl. Energy* **2020**, *279*, 115853. [CrossRef]
123. Thompson, E.P.; Bombelli, E.L.; Shubham, S.; Watson, H.; Everard, A.; D'Ardes, V.; Schievano, A.; Bocchi, S.; Zand, N.; Howe, C.J.; et al. Tinted Semi-Transparent Solar Panels Allow Concurrent Production of Crops and Electricity on the Same Cropland. *Adv. Energy Mater.* **2020**, *10*, 2001189. [CrossRef]
124. Shen, L.; Lou, R.; Park, Y.; Guo, Y.; Stallknecht, E.J.; Xiao, Y.; Rieder, D.; Yang, R.; Runkle, E.S.; Yin, X. Increasing Greenhouse Production by Spectral-Shifting and Unidirectional Light-Extracting Photonics. *Nat Food* **2021**, *2*, 434–441. [CrossRef]
125. Timmermans, G.H.; Hemming, S.; Baeza, E.; van Thoor, E.A.J.; Schenning, A.P.H.J.; Debije, M.G. Advanced Optical Materials for Sunlight Control in Greenhouses. *Adv. Opt. Mater.* **2020**, *8*, 2000738. [CrossRef]
126. Sánchez-Lanuza, M.B.; Menéndez-Velázquez, A.; Peñas-Sanjuan, A.; Navas-Martos, F.J.; Lillo-Bravo, I.; Delgado-Sánchez, J.-M. Advanced Photonic Thin Films for Solar Irradiation Tuneability Oriented to Greenhouse Applications. *Materials* **2021**, *14*, 2357. [CrossRef]
127. Agricultural Adaptation Council. "Waste" Light Can Lower Greenhouse Production Costs. *Greenhouse Canada*, 30 December 2019.
128. Shen, L.; Yin, X. Increase Greenhouse Production with Spectral-Shifting and Unidirectional Light-Extracting Photonics. In Proceedings of the New Concepts in Solar and Thermal Radiation Conversion IV, SPIE, San Diego, CA, USA, 1–5 August 2021; Volume 11824, p. 1182402.
129. Growing Trial for Greenhouse Solar Panels—Research & Innovation | Niagara College. Research & Innovation 2019. Available online: https://www.ncinnovation.ca/blog/research-innovation/growing-trial-for-greenhouse-solar-panels (accessed on 25 October 2021).
130. Chiu, G. Dual Use for Solar Modules. Greenhouse Canada 2019. Available online: https://www.greenhousecanada.com/technology-issues-dual-use-for-solar-modules-32902/ (accessed on 25 October 2021).
131. El-Bashir, S.M.; Al-Harbi, F.F.; Elburaih, H.; Al-Faifi, F.; Yahia, I.S. Red Photoluminescent PMMA Nanohybrid Films for Modifying the Spectral Distribution of Solar Radiation inside Greenhouses. *Renew. Energy* **2016**, *85*, 928–938. [CrossRef]
132. Parrish, C.H.; Hebert, D.; Jackson, A.; Ramasamy, K.; McDaniel, H.; Giacomelli, G.A.; Bergren, M.R. Optimizing Spectral Quality with Quantum Dots to Enhance Crop Yield in Controlled Environments. *Commun. Biol.* **2021**, *4*, 124. [CrossRef]
133. UbiGro A Layer of Light. Available online: https://ubigro.com/case-studies (accessed on 22 September 2021).
134. Kerle Makerspace. Diy Greenhouse by KMS. Download Free STL Model | PrusaPrinters. CC-BY-SA-NC. Available online: https://www.prusaprinters.org/prints/62627-diy-greenhouse-by-kms (accessed on 23 September 2021).
135. CivicSolar, How Does Heat Affect Solar Panel Efficiencies? Available online: https://www.civicsolar.com/article/how-does-heat-affect-solar-panel-efficiencies (accessed on 4 October 2021).
136. Wald, M.L. Why More Solar Panels Should Be Facing West, Not South. *The New York Times*, 1 December 2014.
137. Azzouz, L.; Chen, Y.; Zarrelli, M.; Pearce, J.M.; Mitchell, L.; Ren, G.; Grasso, M. Mechanical Properties of 3-D Printed Truss-like Lattice Biopolymer Non-Stochastic Structures for Sandwich Panels with Natural Fibre Composite Skins. *Compos. Struct.* **2019**, *213*, 220–230. [CrossRef]
138. Mnati, M.J.; Van den Bossche, A.; Chisab, R.F. A Smart Voltage and Current Monitoring System for Three Phase Inverters Using an Android Smartphone Application. *Sensors* **2017**, *17*, 872. [CrossRef] [PubMed]
139. Anand, R.; Pachauri, R.K.; Gupta, A.; Chauhan, Y.K. Design and analysis of a low cost PV analyzer using Arduino UNO. In Proceedings of the 2016 IEEE 1st International Conference on Power Electronics, Intelligent Control and Energy Systems (ICPEICES), Delhi, India, 4–6 July 2016; pp. 1–4.
140. De Anchieta Marques, W.; Ferreira, V.H.; Sotelo, G.G. Design of a real-time, low-cost monitoring system for hybrid solar-wind power generation system. In Proceedings of the 2018 Simposio Brasileiro de Sistemas Eletricos (SBSE), Niteroi, Brazil, 12–16 May 2018; pp. 1–6.
141. Oberloier, S.; Pearce, J.M. Open Source Low-Cost Power Monitoring System. *HardwareX* **2018**, *4*, e00044. [CrossRef]
142. Chen, F.; Wittkopf, S.K.; Khai Ng, P.; Du, H. Solar Heat Gain Coefficient Measurement of Semi-Transparent Photovoltaic Modules with Indoor Calorimetric Hot Box and Solar Simulator. *Energy Build.* **2012**, *53*, 74–84. [CrossRef]
143. Colantoni, A.; Monarca, D.; Marucci, A.; Cecchini, M.; Zambon, I.; Di Battista, F.; Maccario, D.; Saporito, M.G.; Beruto, M. Solar Radiation Distribution inside a Greenhouse Prototypal with Photovoltaic Mobile Plant and Effects on Flower Growth. *Sustainability* **2018**, *10*, 855. [CrossRef]
144. Enokela, J.A.; Othoigbe, T.O. An automated greenhouse control system using Arduino prototyping platform. *Aust. J. Eng. Res.* **2015**, *1*, 64–73. Available online: http://www.mecs-press.org/ijieeb/ijieeb-v9-n3/v9n3-1.html (accessed on 23 September 2021).
145. Vimal, P.V.; Shivaprakasha, K.S. IOT based greenhouse environment monitoring and controlling system using Arduino platform. In Proceedings of the 2017 International Conference on Intelligent Computing, Instrumentation and Control Technologies (ICICICT), Kerala, India, 6–7 July 2017; pp. 1514–1519.
146. Saha, T.; Jewel, M.K.; Mostakim, M.N.; Bhuiyan, N.H.; Ali, M.S.; Rahman, M.K.; Ghosh, H.K.; Hossain, M.K. Construction and development of an automated greenhouse system using Arduino Uno. *Int. J. Inf. Eng. Electron. Bus.* **2017**, *9*, 1. [CrossRef]

147. Siddiqui, M.F.; Kanwal, N.; Mehdi, H.; Noor, A.; Khan, M.A. Automation and monitoring of greenhouse. In Proceedings of the 2017 International Conference on Information and Communication Technologies (ICICT), Karachi, Pakistan, 30–31 December 2017; pp. 197–201.
148. Bedell, R.; Hassan, A.; Tinet, A.-J.; Arrieta-Escobar, J.; Derrien, D.; Dignac, M.-F.; Boly, V.; Ouvrard, S.; Pearce, J.M. Open-Source Script for Design and 3D Printing of Porous Structures for Soil Science. *Technologies* **2021**, *9*, 67. [CrossRef]
149. Jaiganesh, S.; Gunaseelan, K.; Ellappan, V. IOT Agriculture to Improve Food and Farming Technology. In Proceedings of the 2017 Conference on Emerging Devices and Smart Systems (ICEDSS), Mallasamudram, India, 3–4 March 2017; pp. 260–266.
150. Kassim, M.R.M. IoT Applications in Smart Agriculture: Issues and Challenges. In Proceedings of the 2020 IEEE Conference on Open Systems (ICOS), Kota Kinabalu, Malaysia, 17–19 November 2020; pp. 19–24.